



**HAL**  
open science

# Synthesis and self-assembly of AB<sub>2</sub>-type amphiphilic copolymers from biobased hydroxypropyl methyl cellulose and poly(L-lactide)

Aijing Lu, Jielin Wang, Marleny Caceres Najarro, S.M. Li, André Deratani

## ► To cite this version:

Aijing Lu, Jielin Wang, Marleny Caceres Najarro, S.M. Li, André Deratani. Synthesis and self-assembly of AB<sub>2</sub>-type amphiphilic copolymers from biobased hydroxypropyl methyl cellulose and poly(L-lactide). *Carbohydrate Polymers*, 2019, 211, pp.133-140. 10.1016/j.carbpol.2019.01.110 . hal-02076331

**HAL Id: hal-02076331**

<https://hal.umontpellier.fr/hal-02076331v1>

Submitted on 21 Oct 2021

**HAL** is a multi-disciplinary open access archive for the deposit and dissemination of scientific research documents, whether they are published or not. The documents may come from teaching and research institutions in France or abroad, or from public or private research centers.

L'archive ouverte pluridisciplinaire **HAL**, est destinée au dépôt et à la diffusion de documents scientifiques de niveau recherche, publiés ou non, émanant des établissements d'enseignement et de recherche français ou étrangers, des laboratoires publics ou privés.



Distributed under a Creative Commons Attribution - NonCommercial 4.0 International License

1            Synthesis and Self-Assembly of AB<sub>2</sub>-type Amphiphilic Copolymers from Biobased  
2                            Hydroxypropyl Methyl Cellulose and Poly(L-lactide)

3  
4            Aijing Lu, Jieli Wang, Marleny Caceres Najarro, Suming Li\*, Andre Deratani

5            Institut Européen des Membranes, UMR CNRS 5635, Université de Montpellier, Place  
6                            Eugene Bataillon, 34095 Montpellier Cedex 5, France

7  
8            **Abstract:** AB<sub>2</sub>-type amphiphilic (HPMC)<sub>2</sub>-PLA copolymers with various hydrophilic  
9 block lengths were synthesized using a three step procedure: ring-opening polymerization of  
10 L-lactide initiated by propynol, amination reduction of the aldehyde endgroup of HPMC, and  
11 thiol-click reaction. The resulted copolymers were characterized by NMR, DOSY-NMR, SEC  
12 and FT-IR. The cloud point (CP) was determined by UV–visible spectrometer. Data show that  
13 the HPMC block length has little effect on the Cp of the copolymers which is lower than that  
14 of HPMC. The self-assembly behavior of the copolymers was investigated from DLS, TEM,  
15 and critical micelle concentration (CMC) measurements. Spherical micelles are obtained by  
16 self-assembly of copolymers in aqueous solution. The micelle size and the CMC of  
17 copolymers increase with increasing HPMC block length. It is concluded that biobased and  
18 biodegradable (HPMC)<sub>2</sub>-PLA copolymers could be promising as nano-carrier of hydrophobic  
19 drugs.

20  
21    \* Corresponding authors: [suming.li@umontpellier.fr](mailto:suming.li@umontpellier.fr) (S. Li)

23

## 24 1. Introduction

25        Micelles based on amphiphilic block copolymers have been extensively investigated as  
26 drug carrier due to their favorable advantages in molecular design, long circulation, enhanced  
27 drug loading and therapeutic effect, and biocompatibility (Kataoka, Harada, & Nagasaki,  
28 2001). Thus, biocompatible and bioresorbable aliphatic polyesters such as polylactide (PLA),  
29 polyglycolide (PGA), poly(lactide-co-glycolide) (PLGA), and poly( $\epsilon$ -caprolactone) (PCL)  
30 have been commonly used as the hydrophobic block, whereas poly(ethylene glycol) (PEG),  
31 poly(N-vinyl-2-pyrrolidone) (PVP), poly(N-isopropylacrylamide) (PNIPAAm), poly(vinyl  
32 alcohol) (PVA), poly(amino acid), and more recently polysaccharides as the hydrophilic block  
33 to construct amphiphilic block copolymers (Elsabahy & Wooley, 2012; Guo, Wang, Shen,  
34 Shu, & Sun, 2013; Mi, Wang, Nishiyama, & Cabral, 2017; Yi et al., 2018). PLA, as an FDA-  
35 approved biobased polyester, is widely used in biomedical and pharmaceutical fields in the  
36 form of drug carrier, tissue engineering scaffolds, bone fracture internal fixation devices,  
37 orthopedic screws and plates, etc, due to its good degradability, processability, and  
38 mechanical strength (Lassalle & Ferreira, 2007; Rajendra P. Pawara & Abraham J. Dombb,  
39 2014; Ramzi A. Abd Alsaheb, 2015; Rancan et al., 2009; Saini, Arora, & Kumar, 2016; Tsuji,  
40 2005). Interestingly, PLA stereocomplex has been used to construct colloidal systems such as  
41 mixed micelles and hydrogels for pharmaceutical applications (L. Yang, Wu, Liu, Duan, & Li,  
42 2009).

43        PEG is also an FDA-approved polymer widely used for biomedical and pharmaceutical  
44 applications. Nevertheless, PEG as a polyether is prone to peroxidation, which could

45 adversely affect cells (Barz, Luxenhofer, Zentel, & Vicent, 2011; Ishida & Kiwada, 2008).  
46 Therefore, great effort has been made to search for hydrophilic alternatives of PEG.  
47 Polysaccharides have attracted increasing attention in recent years for uses as biomaterials to  
48 solve problems related to immunogenicity and toxicity associated with synthetic polymers  
49 because of their biodegradability, biocompatibility and bio-based nature (Aminabhavi,  
50 Nadagouda, Joshi, & More, 2014; Ganguly, Chaturvedi, More, Nadagouda, & Aminabhavi,  
51 2014). Certain polysaccharides present inherent bioactivity that can help in mucoadhesion,  
52 thus improving drug targeting and diminishing inflammatory response. Recent years have  
53 witnessed a rapid growth on polysaccharide based micelles as drug delivery system  
54 (Aminabhavi et al., 2014; Rudzinski & Aminabhavi, 2010), such as pullulan (Jeong et al.,  
55 2006), cellulose (Guo, Wang, Shu, Shen, & Sun, 2012), dextran (Jeong et al., 2011; Sun et al.,  
56 2009), chitosan (Huo et al., 2012), heparin (Tian et al., 2010), and hyaluronan (Y. L. Yang,  
57 Kataoka, & Winnik, 2005). Among them, cellulose is of great importance because of its  
58 outstanding properties, but its applications are restrained due to its poor solubility. Thus,  
59 soluble cellulose derivatives have been studied as a hydrophilic building block to prepare  
60 amphiphilic copolymers which can self-assemble in micelles, such as ethyl cellulose,  
61 hydroxyl propyl cellulose (Ostmark, Nystrom, & Malmstrom, 2008), hydroxyl propyl methyl  
62 cellulose (HPMC) (Ostmark et al., 2008), hydroxyl ethyl cellulose (Hsieh, Van Cuong, Chen,  
63 Chen, & Yeh, 2008) etc. Graft copolymerization of PLA onto cellulose and cellulose  
64 derivatives have been reported (Chen & Sun, 2000; Teramoto & Nishio, 2003; Yuan, Yuan,  
65 Zhang, & Xie, 2007). However, the grafting of PLA on the side chain hydroxyl group results  
66 in complex chain structure and the reaction is poorly controllable.

67 In our previous work (Wang, Caceres, Li, & Deratani, 2017), linear HPMC-*b*-PLA  
68 diblock copolymers with various HPMC block lengths were synthesized by combination of  
69 ring-opening polymerization, amination reduction and thiol-click reaction. The resulted  
70 amphiphilic copolymers are susceptible to self-assemble into spherical micelles with a  
71 diameter of 60-120 nm. It has been shown that the geometrical structure of copolymers affect  
72 the morphology, stability and size of micelles because the hydrophobic and hydrophilic  
73 segments lead to complex spatial arrangements during the micellization process (Cao et al.,  
74 2013; Li, Kesselman, Talmon, Hillmyer, & Lodge, 2004). In this work, amphiphilic AB<sub>2</sub>-type  
75 PLA-(HPMC)<sub>2</sub> copolymers with various HPMC molar masses were synthesized and  
76 characterized. The self-assembly properties of the copolymers were investigated from the  
77 morphology, size and size distribution, cloud point (C<sub>p</sub>) and critical micelle concentration  
78 (CMC) measurements.

79

## 80 2. Materials and Methods

### 81 2.1 Materials

82 L-lactide was purchased from Purac Biochem (Goerinchem, Netherlands) and purified  
83 by recrystallization from ethyl acetate. HPMC (K4M) was kindly provided by Colorcon-Dow  
84 chemical (Bougival, France). Propynol, stannous octoate (Sn(Oct)<sub>2</sub>), cysteamine, sodium  
85 cyanoborohydride (NaBH<sub>3</sub>CN), 1,4-dithiothreito (DTT), 2,2-dimethoxy-2-  
86 phenylacetophenone (DMPA), diethyl ether and dimethyl sulfoxide were purchased from  
87 Sigma-Aldrich, and used as received. Toluene was purchased from Sigma-Aldrich, dried over  
88 by calcium chloride (CaCl<sub>2</sub>) and distilled prior to use.

## 89 2.2 Synthesis of alkynyl terminated PLLA

90 Alkynyl terminated PLLA was synthesis by ring-open polymerization, of L-lactide using  
91 propynol as initiator and Sn(Oct)<sub>2</sub> as catalyst. Typically, L-lactide (7.2 g), propynol (0.112 g),  
92 and Sn(Oct)<sub>2</sub> (0.2 g) were introduced into a dried Schlenk tube, and 30 mL anhydrous toluene  
93 was added under stirring. The solution was degassed by performing five freeze–pump–thaw  
94 cycles. The reaction then proceeded 24 h at 80°C. Finally the product was obtained by  
95 precipitation in methanol, followed by vacuum drying.

## 96 2.3 Enzymatic degradation of HPMC and determination of substitution degree

97 HPMC was depolymerized to yield HPMC oligomers as reported in a previous work  
98 (Wang et al., 2017). Briefly, 1 g HPMC was added in 100 mL citrate phosphate buffer (pH =  
99 5), and stirred overnight at 47 °C to ensure complete dissolution. Cellulase was added to the  
100 solution, and enzymatic depolymerization proceeded for various time periods. The reaction  
101 was stopped by heating the solution to 85 °C, and the suspension was hot filtrated. The  
102 collected solution was purified by dialysis for 3 days using a membrane of MWCO=3500 g  
103 mol<sup>-1</sup>, followed by freeze drying.

104 HPMC is a cellulose derivative whose hydroxyl groups are substituted by methyl and  
105 hydroxypropyl groups. The average number of substituents per repeat unit is characterized by  
106 the molar substitution or hydroxypropylation ( $MS_{HP}$ ) and the degree of substitution or  
107 methylation ( $DS_{Me}$ ). The former can be higher than 3 and the latter varies between 0 and 3.  
108 HPMC with a  $DS_{Me}$  between 0.1 and 2.0 is water soluble as the substitution groups allow to  
109 decrease the intra- and inter-chain hydrogen bonding. In contrast, when the DS is above 2,  
110 HPMC becomes insoluble in water due to the presence of many hydrophobic methyl groups.

111 (Claes, 2006). The  $^1\text{H}$  NMR spectra of acetylated HPMC oligomers were acquired in  $\text{CDCl}_3$   
112 at 50 °C. The  $\text{DS}_{\text{Me}}$  and  $\text{MS}_{\text{HP}}$  values were then calculated according to the method reported  
113 by Fitzpatrick (Fitzpatrick et al., 2006).

114

#### 115 2.4 Synthesis of thiol terminated HPMC

116 Thiol terminated HPMC was obtained by reductive amination connecting the aldehyde  
117 end group of HPMC molecules and the amine group of cysteamine in the presence of sodium  
118 cyanoborohydride. Briefly, HPMC with  $\text{DS}_{\text{Me}}$  of 1.43 and average molar mass of 7000 g  
119  $\text{mol}^{-1}$  (1 g) and  $\text{NaBH}_3\text{CN}$  (0.2 g) were solubilized in a mixture (3/1 v/v) of 50 mL dimethyl  
120 sulfoxide (DMSO) and 0.01 M NaCl at 60 °C. Cysteamine (0.1 g) was added, and the solution  
121 was stirred at 60 °C for 6 days under reflux. The solution was then dialyzed against deionized  
122 water for 3 days ( $\text{MWCO}$  3500  $\text{g mol}^{-1}$ ), followed by freeze drying. Afterwards, the product  
123 was dissolved in water, and stirred overnight in the presence of excess DTT under nitrogen  
124 atmosphere. Finally, the solution was dialyzed against deionized water and freeze dried.  
125 Ellman assay was performed to determine the content of thiol group using 5,5'-dithio-bis-(2-  
126 nitrobenzoic acid) (DTNB) as Ellman's reagent. DTNB is a versatile water soluble compound  
127 for quantitating free sulfhydryl groups as a measurable yellow-colored product is formed  
128 when DTNB reacts with sulfhydryl in solution.

#### 129 2.5 Synthesis of $(\text{HPMC})_2$ -*b*-PLLA

130 Amphiphilic block copolymers were synthesized by thiol-yne click reaction connecting  
131 thiol terminated HPMC and alkynyl terminated PLLA. The reaction was initiated in a Dinics  
132 M3 UV chamber equipped with a PL-L 36 W/01/4P Hg Lamp. Typically, thiol terminated

133 HPMC (1.0 g), alkynyl terminated PLLA (0.15 g), and DMPA (0.013 g) were dissolved in 10  
134 mL DMSO. The solution was degassed for 30 min using purified argon, and then subjected  
135 to UV irradiation for 5 h. The crude product was collected by precipitation in acetonitrile,  
136 followed by centrifugation at 4500 rpm for 15 min. The above dissolution–precipitation  
137 cycle was repeated twice. Finally, (HPMC)<sub>2</sub>-*b*-PLLA copolymers were obtained as a white  
138 solid after vacuum drying.

## 139 2.6 Characterization

140 <sup>1</sup>H NMR spectra were recorded on Bruker spectrometer operating at 300 MHz  
141 (AMX300) using CDCl<sub>3</sub> and DMSO-*d*<sub>6</sub> as solvent. Diffusion ordered spectroscopy (DOSY)  
142 NMR was performed on Bruker Avance (AQS600) NMR spectrometer, operating at 600 MHz  
143 and equipped with a Bruker multinuclear z-gradient inverse probe head which is able to  
144 produce gradients in the z direction with the strength of 55 Gcm<sup>-1</sup>. The DOSY spectra were  
145 acquired from Bruker topspin software (version 2.1) with the ledbpgp2s pulse program. The  
146 strength of the pulsed field gradients with respect to maximum 32 increments on a quadratic  
147 scale was logarithmically incremented from 2 to 95%. The diffusion sensitive period ( $\Delta$ ) of  
148 200 ms and the gradient duration ( $\delta$ ) of 5 ms were optimized to allow the signals of interest to  
149 decrease by a factor of 10–20, in order to keep the relaxation contribution to the signal  
150 attenuation constant and ensure full signal attenuation for all samples. Data were processed  
151 using the MestRe Nova software.

152 Size exclusion chromatography (SEC), equipped with MALLS in combination with  
153 refractive index (RI) detection allows to determine the absolute molar mass of polymers. 5 mg  
154 of samples were added in the mobile phase (0.01 M NaCl containing 0.02% NaN<sub>3</sub>), and



155 stirred for 24 h at room temperature. The solution was filtered using 0.45  $\mu\text{m}$   
156 polytetrafluoroethylene (PTFE) filter (Millipore). The filtrate was injected through a 100  $\mu\text{L}$   
157 loop (Rheodyne injector 7725), and eluted on a TSK-GEL GMPWXL 7.8 $\times$ 300 mm column  
158 (TosoHaas Bioseparation Specialists, Stuttgart, Germany) at a flow rate of 0.5  $\text{mL min}^{-1}$   
159 (Waters pump 515). MALS detector (Dawn DSP, Wyatt Technology Co, Santa Barbara, CA,  
160 USA) and RI detector (Optilab Wyatt Technology Co) were used to online determine the  
161 absolute molar mass for each elution fraction of 0.01 mL, which enables to calculate the  
162 weight average molar mass ( $M_w$ ) and the dispersity ( $\text{Đ} = M_w/M_n$ ). The refractive index  
163 increment ( $dn/dc$ ) for calculation was 0.137  $\text{mL g}^{-1}$ . Data analysis was realized using Astra 4  
164 (Wyatt Technology Co).

165 Fourier transform infrared (FT-IR) spectra were recorded on a Nicolet NEXUS  
166 spectrometer with a DTGS detector at 4  $\text{cm}^{-1}$  resolution. 64 scans were taken per sample in  
167 the frequency range from 400 to 4000  $\text{cm}^{-1}$ . Sample pellets were prepared by mixing 2–2.5  
168 mg of polymer with 200 mg of spectral grade potassium bromide, followed by compression  
169 using a press.

170 The cloud point ( $C_p$ ) of the copolymers was estimated from transmittance changes of  
171 copolymer solutions in the temperature range from 30 to 90 $^{\circ}\text{C}$ . The solution at 3.0  $\text{mg mL}^{-1}$   
172 was stirred for 24 h and kept at 5  $^{\circ}\text{C}$  overnight before analysis. Measurements were made at a  
173 wavelength of 600 nm with a Perkin Elmer Lambda 35 UV–visible spectrometer equipped  
174 with a Peltier temperature programmer PTP-1+1. The temperature ramp was 0.1  $^{\circ}\text{C min}^{-1}$ .  
175 Temp Lab software was used for data treatment.

176 Dynamic light scattering (DLS) was performed at 25 $^{\circ}\text{C}$  with 90 $^{\circ}$  scattering angle using

177 Zano-ZS (Malvern Instrument) equipped with a He–Ne laser ( $\lambda = 632.8$  nm). The aqueous  
178 solutions of copolymers at  $1.0 \text{ mg mL}^{-1}$  were filtered through a  $0.45 \text{ }\mu\text{m}$  PTFE microfilter  
179 before measurements. The correlation of the distribution of diffusion coefficient ( $D$ ) was  
180 analyzed via the general purpose method (non-negative least squares). The apparent  
181 equivalent hydrodynamic radius ( $R_H$ ) was obtained using the cumulate method from the  
182 Stoke–Einstein equation.

183 The critical micelle concentration (CMC) of copolymers was determined using an  
184 autocorrelation function according to the methodology proposed by Muller et al (Muller et al.,  
185 2015). Aqueous solutions of copolymers were prepared in deionized water at concentrations  
186 ranging from  $0.006$  to  $1.0 \text{ g L}^{-1}$ , and were incubated overnight. The scattering intensity of the  
187 solutions was measured at  $25 \text{ }^\circ\text{C}$  with a Malvern Instrument Nano-ZS. The scattering intensity  
188 proportional to the size and number of objects present in the solution was recorded. The CMC  
189 was taken as the intersection of regression lines from the plots of the scattering intensity  
190 against the polymer concentration.

191 Transmission electron microscopy (TEM) was performed on JEOL 1200 EXII  
192 instrument, operating at an acceleration voltage of  $120 \text{ kV}$ .  $5 \text{ }\mu\text{L}$  of micellar solution at  $1.0 \text{ mg}$   
193  $\text{mL}^{-1}$  were dropped onto a carbon coated copper grid, and air dried before measurements.

194

### 195 3. Results and Discuss

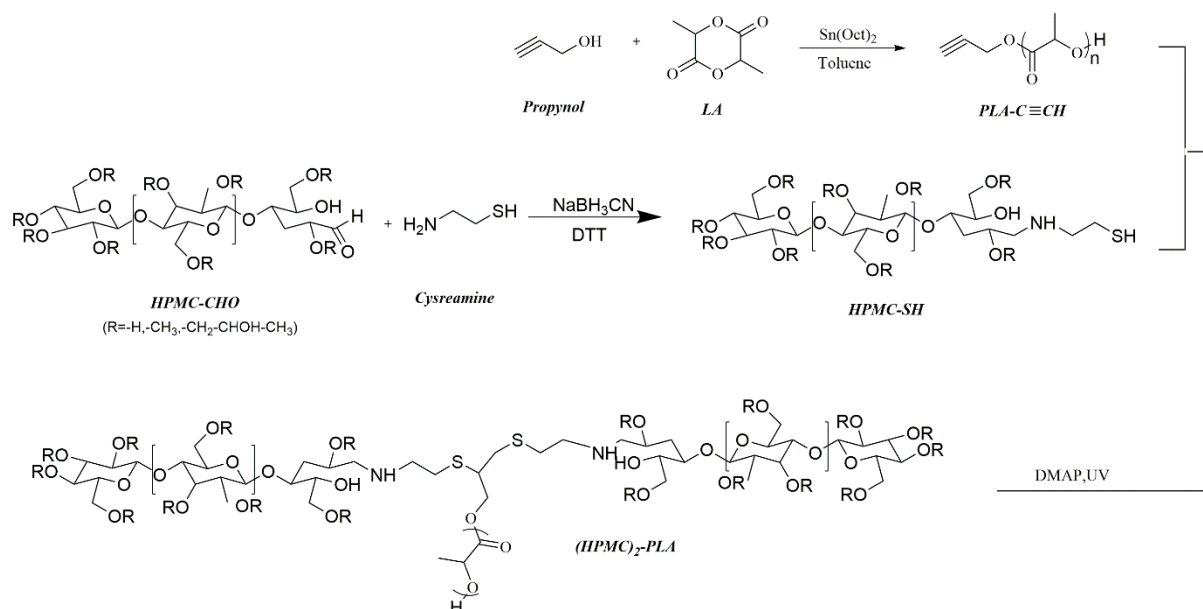
#### 196 3.1 Synthesis of amphiphilic block copolymers

197 HPMC was depolymerized by using cellulase to yield oligomers with various molar  
198 masses. The weight average molar mass ( $M_w$ ) of the resulted HPMC oligomers was  $5000$ ,

199 7000 and 10000 Daltons, respectively, as determined by SEC. The NMR spectra of acetylated  
 200 HPMC were recorded in CDCl<sub>3</sub> (Figure S1). The DS<sub>Me</sub> and MS<sub>HP</sub> were calculated according  
 201 to the method reported by Fitzpatrick (Table S1). The DS<sub>Me</sub> varies from 1.17 to 1.43, indicating  
 202 that HPMC samples are water soluble.

203 The synthesis of (HPMC)<sub>2</sub>-*b*-PLA copolymers was achieved in three steps (Scheme 1):  
 204 a) synthesis of alkynyl terminated PLLA, b) thiolation of HPMC, and c) UV-initiated thiol-  
 205 yne click reaction between thiolated HPMC and alkynyl terminated PLLA.

206



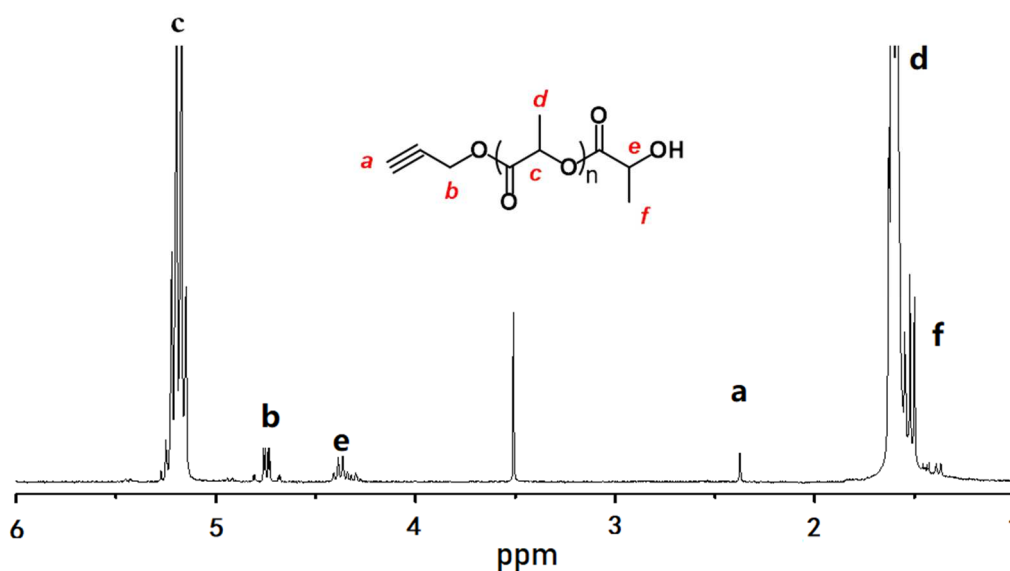
207

208 Scheme 1. Synthesis route of (HPMC)<sub>2</sub>-*b*-PLA block copolymers

209

210 Alkynyl terminated PLLA was synthesized by ring-opening polymerization of L-lactide  
 211 using propynol as initiator with a monomer/initiator molar ratio of 25/1. Figure 1 shows the  
 212 <sup>1</sup>H NMR spectrum of the resulting alkynyl terminated PLLA. The signals at 2.4 (a) and 4.75  
 213 (b) ppm are assigned to the alkynyl group and the methylene groups adjacent to the alkynyl  
 214 group, respectively. The signals at 1.62 (d) and 5.25 (c) ppm are assigned to the methyl and

215 methyne protons of PLA main chain, and the signals at 1.50 (f) and 4.42 (e) ppm to methyl  
216 and methyne protons of the hydroxyl terminal unit. The polymerization degree (DP) of PLA  
217 calculated from the integration ratio of signals c to e was 28, corresponding to a number  
218 average molar mass ( $M_{n,NMR}$ ) of about 2000 g/mol.



219

220 Figure 1. NMR spectrum of alkynyl-terminated PLA in  $CDCl_3$

221

222 Thiol terminated HPMC was obtained by reductive amination of HPMC with  
223 cysteamine. The molecular chain of cellulose has a non reducing group at one end, and a  
224 hemiacetal group at the other end. The latter is a reducing group which can be easily  
225 converted to aldehyde group (Schatz & Lecommandoux, 2010). The amine functional group  
226 of cysteamine reacted with the unique aldehyde endgroup of HPMC through reductive  
227 amination to yield HPMC-S-S-HPMC together with small amounts of unreacted HPMC,  
228 HPMC-SH, and HPMC-S-S-( $CH_2$ )<sub>6</sub>-NH<sub>2</sub>. HPMC-S-S-HPMC was then reduced using DTT to  
229 yield HPMC-SH (Wang et al., 2017). The final product was characterized by using Ellman  
230 assay and SEC measurement. Ellman's assay showed that the content of thiol terminated

231 HPMC in the final product was 88%. SEC confirmed that the final product is predominantly  
232 composed of HPMC-SH because its  $M_w$  is almost the same as that of the initial HPMC. These  
233 findings showed that thiol terminated HPMC was successfully synthesized.

234 Finally amphiphilic block copolymers were obtained by UV-initiated thiol-yne click  
235 reaction between thiol terminated HPMC and alkynyl terminated PLLA. Three copolymers,  
236 namely (HPMC5K)<sub>2</sub>-PLA2K, (HPMC7K)<sub>2</sub>-PLA2K and (HPMC10K)<sub>2</sub>-PLA2K were  
237 synthesized using the same hydrophobic PLA block with  $M_n$  of 2000 g mol<sup>-1</sup> and different  
238 hydrophilic HPMC-SH blocks with  $M_w$  of 5000, 7000, and 10000 g mol<sup>-1</sup>, respectively.  
239 Figure 2 shows the <sup>1</sup>H NMR spectra of (HPMC7K)<sub>2</sub>-PLA2K copolymer in D<sub>2</sub>O and DMSO-  
240 *d*<sub>6</sub>. The spectrum in DMSO-*d*<sub>6</sub> shows the signal at 1.05 ppm (a) corresponding to the methyl  
241 protons in the hydroxypropyl group, and those in the range of 2.75–4.75 ppm (b) to the  
242 methyl protons adjacent to the oxygen moieties of the ether linkages, inner methylene and  
243 methine protons and HPMC backbone protons (Figure 2A). The signals at 1.49 (d) and 5.24  
244 ppm (c) belong to the methyl and methine protons of PLLA blocks. Moreover, the signal  
245 detected at 2.3 ppm is assigned to the methylene group of the connecting unit. These results  
246 confirm the successful synthesis of copolymers by thiol-yne click reaction.

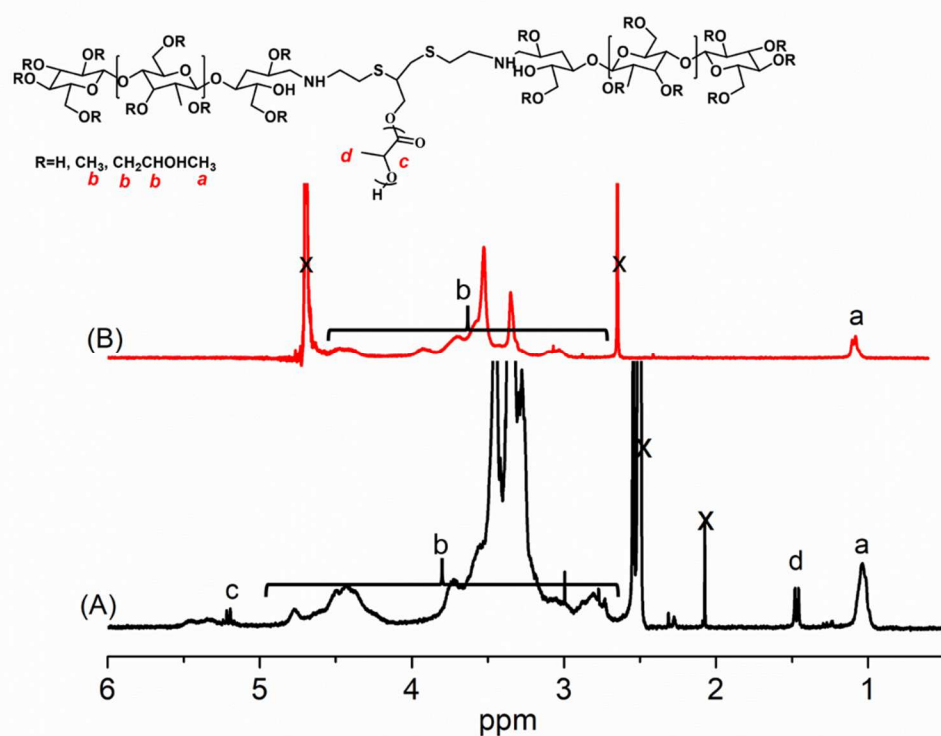


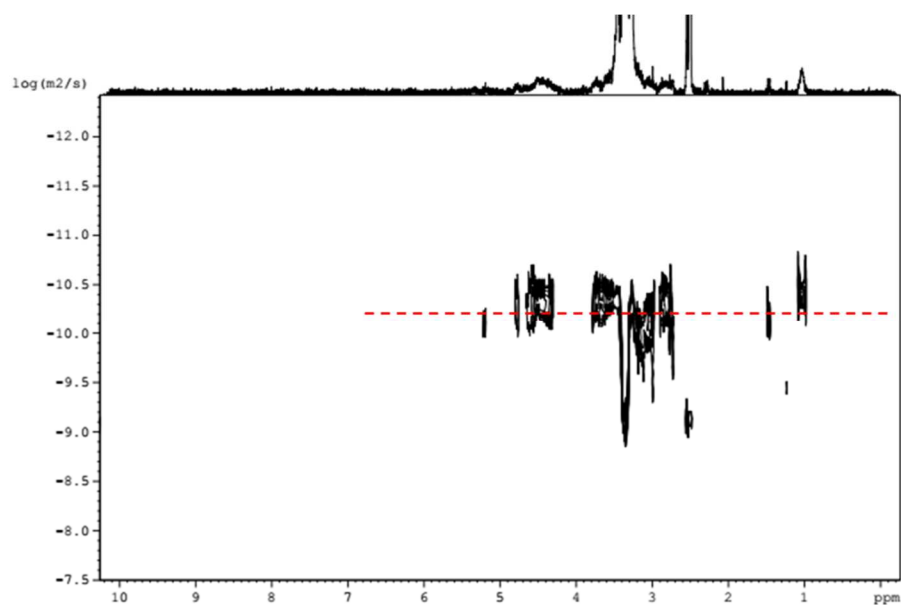
Figure 2.  $^1\text{H}$  NMR spectra of  $(\text{HPMC})_2\text{-PLA}$  in  $\text{DMSO-d}_6$  (A) and in  $\text{D}_2\text{O}$  (B)

247

248

249

250 The structure of block copolymers was also confirmed by DOSY-NMR. DOSY is an  
 251 excellent tool commonly used for the analysis of complex mixtures as it allows virtual  
 252 separation of multicomponent systems. DOSY-NMR data are presented in a two-dimensional  
 253 (2D) pattern: one dimension is related to the chemical shift information, and the other  
 254 represents the diffusion coefficient which reflects the molecular effective sizes (Pages, Gilard,  
 255 Martino, & Malet-Martino, 2017). As shown in Figure 3, the signals of both PLA and HPMC  
 256 components present the same diffusion coefficient, which indicates that the two blocks are  
 257 attached in one molecule. In other words, the copolymer was effectively synthesized.

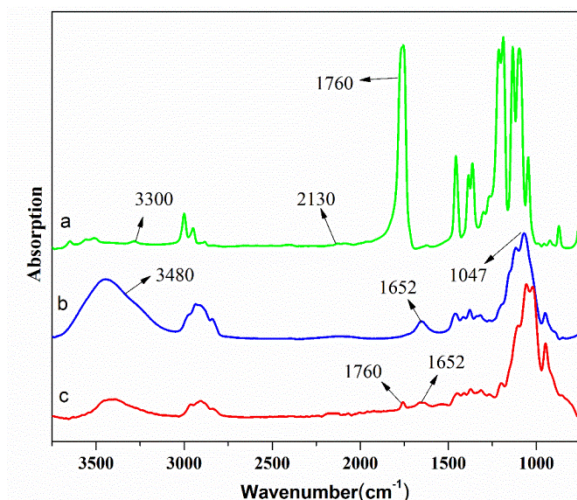


258

259 Figure 3. DOSY NMR spectrum of (HPMC7K)<sub>2</sub>-PLA2K copolymer in DMSO-*d*<sub>6</sub> at 298 K

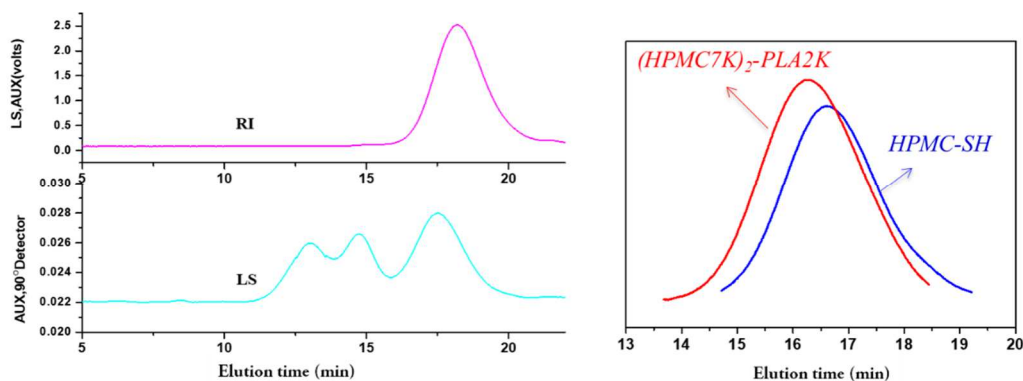
260

261 FT-IR is also used to examine the structure of copolymers. Figure 4 presents the FT-IR  
 262 spectra of alkynyl terminated PLLA, thiol terminated HPMC, and (HPMC7K)<sub>2</sub>-PLA2K  
 263 copolymer. Alkynyl terminated PLLA presents characteristic absorption bands at 1760, 2130  
 264 and 3300 cm<sup>-1</sup> belonging to the carbonyl group, and alkynyl group, respectively. Thiol  
 265 terminated HPMC presents an amide adsorption band at 1652 cm<sup>-1</sup>, a strong C-O absorption  
 266 band at 1047 cm<sup>-1</sup>, and a broad O-H stretching vibration band at 3480 cm<sup>-1</sup>. (HPMC)<sub>2</sub>-b-PLA  
 267 shows the characteristic bands from both components, in agreement with the successful  
 268 coupling of PLLA and HPMC blocks.



269  
 270 Figure 4. FT-IR spectra of (a) alkynyl terminated PLLA, (b) thiol terminated HPMC, and (c)  
 271 (HPMC7K)<sub>2</sub>-PLA2K copolymer.  
 272

273 The molar mass of the copolymers was determined by SEC in conjunction with online  
 274 light scattering and refractive index (RI) detectors, as shown in Figure 5. RI detector is most  
 275 commonly used as concentration detector whose response is proportional to the total solute  
 276 concentration in the detector cell. Meanwhile, the response of multi-angle laser light  
 277 scattering (MALLS) detector depends on the molar mass of a polymer in the detector cell  
 278 (Kostanski, Keller, & Hamielec, 2004). Combination of the two curves allows to determine  
 279 the weight average molar mass of copolymers.



280  
 15



281 Figure 5. Refractive index and light scattering curves of (HPMC7K)<sub>2</sub>-PLA2K (left), and SEC  
 282 curves of HPMC-SH and (HPMC7K)<sub>2</sub>-PLA2K in water

283

284 The  $M_w$  and dispersity data of the three copolymers are summarized in Table 1. The  $M_w$   
 285 ranges from 12000 for (HPMC5K)<sub>2</sub>-PLA2K to 22 0000 g mol<sup>-1</sup> for (HPMC10K)<sub>2</sub>-PLA2K. It  
 286 is noted that the  $M_w$  of the copolymers well agrees with the sum of the molar masses of both  
 287 components although the value of  $M_n$  is used for PLA. Meanwhile, the dispersity ( $\mathcal{D}=M_w/M_n$ )  
 288 ranges from 1.13 to 1.26, in agreement with narrow molar mass distribution of copolymers.

289

290 Table 1. Characterization of (HPMC)<sub>2</sub>-PLA copolymers

291

| Sample                        | $M_{w, SEC}^a)$<br>(g/mol) | $\mathcal{D}^a)$ | $C_p^b)$<br>(°C) | CMC <sup>c)</sup><br>(mg/mL) | $R_h^{d)}$<br>(nm) | PDI <sup>d)</sup> |
|-------------------------------|----------------------------|------------------|------------------|------------------------------|--------------------|-------------------|
| (HPMC10K) <sub>2</sub> -PLA2K | 22000                      | 1.26             | 65.2             | 0.16                         | 120                | 0.21              |
| (HPMC7K) <sub>2</sub> -PLA2K  | 16000                      | 1.24             | 64.8             | 0.15                         | 90                 | 0.12              |
| (HPMC5K) <sub>2</sub> -PLA2K  | 12000                      | 1.13             | 64.1             | 0.14                         | 66                 | 0.19              |

292

293 a) Determined from SEC/MALS/RI measurement in water at 5.0mg mL<sup>-1</sup>

294

294 b) Determined from turbidimetry measurement in water at 20.0 mg mL<sup>-1</sup>

295

295 c) Determined at 25°C by dynamic light scattering

296

296 d) Determined at 25°C by dynamic light scattering at 1.0 mg mL<sup>-1</sup>

297

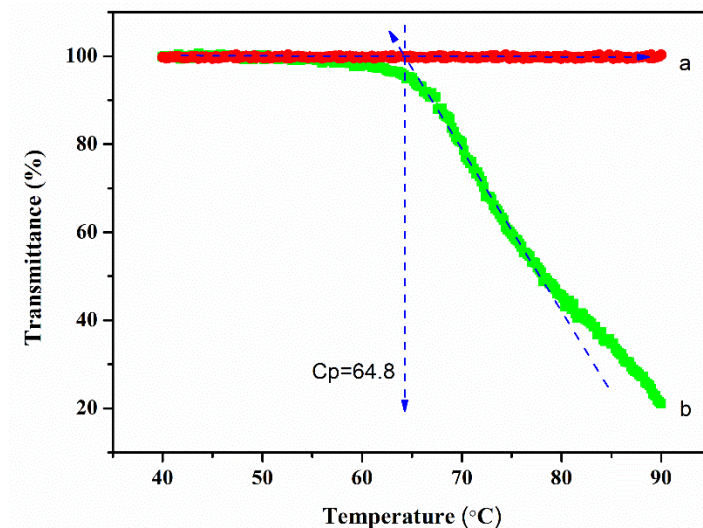
### 298 3.2. Cloud point of (HPMC)<sub>2</sub>-PLA copolymers

299 The cloud point ( $C_p$ ), also named lower critical solution temperature (LCST), is  
 300 considered as the solubility limit of amphiphiles due to phase-separation as the temperature  
 301 increases. In fact, the hydrogen bonding between polymer chains and surrounding water

302 molecules weakens when the temperature approaches the cloud point, leading to decrease of  
303 the polymer solubility and phase separation. Thus the polymer precipitates out of solution as a  
304 consequence of equal chemical potentials between the two phases: one is rich in polymer, and  
305 the other rich in solvent (Sardar, Kamil, Kabir ud, & Sajid Ali, 2011).

306 Figure 6 shows the transmittance changes of (HPMC7K)<sub>2</sub>-PLA2K solutions at 3.0  
307 mg/mL, in comparison with HPMC7K homopolymer. The two solutions initially exhibit a  
308 transmittance close to 100%. With increasing temperature, the transmittance of HPMC7K  
309 remained almost unchanged till 90°C. This indicates that HPMC oligomers are not thermos-  
310 responsive in this temperature range, in contrast to high molar mass HPMC (Sardar et al.,  
311 2011). Interestingly, (HPMC7K)<sub>2</sub>-PLA2K exhibits a decrease of light transmittance to nearly  
312 20% from about 60°C up to 90 °C. The clouding at a given temperature results from the  
313 destruction of hydrogen bonding between water and HPMC molecules leading to phase  
314 separation (Khan, Anjum, Koya, Qadeer, & Kabir ud, 2014). The Cp value was determined by  
315 extrapolation of the linear region of 100% of transmittance and tangent line of the inflexion  
316 point. A Cp value of 64.8°C is obtained for (HPMC7K)<sub>2</sub>-PLA2K. Similarly, Cp values of 65.2  
317 and 64.1°C are obtained for (HPMC10K)<sub>2</sub>-PLA2K and (HPMC5K)<sub>2</sub>-PLA2K (Table 1).  
318 Therefore, the length of HPMC blocks has little effect on the Cp value of the copolymers.  
319 Similar results have been previously reported in literature for poly(lactide-*b*-*N*-  
320 isopropylacrylamide-*b*-lactide) (PLA-*b*-PNIPAAm- *b*-PLA) triblock copolymers (You, Hong,  
321 Wang, Lu, & Pan, 2004). In fact, a Cp value of about 31°C was obtained for copolymers with  
322 PLA/PNIPAAm ratios of 1.0/1.9, 1.0/3.0 and 1.0/3.6.

323



324  
 325 Figure 6. Transmittance changes of HPMC7K (a) and (HPMC7K)<sub>2</sub>-PLA2K (b) solutions at  
 326 3.0 mg/mL as a function of temperature.

327  
 328 In our previous work, the phase separation behavior of linear HPMC-*b*-PLA diblock  
 329 copolymers with different HPMC block lengths (HPMC5K-PLA2K, HPMC8K-PLA2K, and  
 330 HPMC10K-PLA2K) was investigated (Wang et al., 2017). All copolymers exhibit a slow  
 331 decrease of light transmittance from 55 to 80 °C. Beyond, a sharper decrease of transmittance  
 332 down to 78% is detected. The three diblock copolymers exhibit almost the same  $C_p$  values of  
 333 *c.a.* 80°C. Therefore, the length of HPMC blocks has little effect on the  $C_p$ , but the copolymer  
 334 topology seems to significantly affect the phase separation behavior of HPMC-*b*-PLA  
 335 copolymers. It has been reported that the cloud point was elevated by more than 40 °C  
 336 through the linear-to-cyclic topological conversion of the polymer amphiphiles (Honda,  
 337 Yamamoto, & Tezuka, 2010).

338  
 339 3.3. Self-assembly of (HPMC)<sub>2</sub>-PLA copolymers

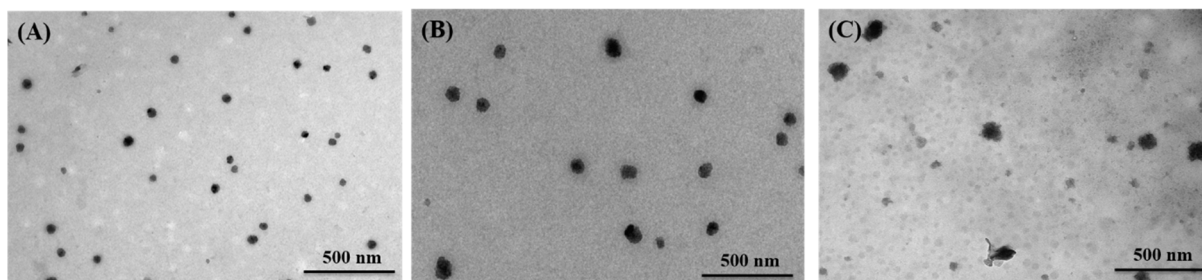
340 The self-assembly properties of (HPMC)<sub>2</sub>-PLA copolymers were investigated to evaluate

341 their potential as drug carrier. NMR provides a means to analyze the self-assembly behavior  
342 of amphiphilic block copolymers in solvents which can dissolve one of the two blocks only.  
343 Figure 2(B) shows the  $^1\text{H}$  NMR spectrum of (HPMC7K)<sub>2</sub>-PLA2K copolymer in deuterated  
344 water (D<sub>2</sub>O). Different from DMSO-*d*<sub>6</sub> which is a good solvent for both HPMC and PLLA,  
345 D<sub>2</sub>O only solubilizes hydrophilic HPMC segments. Therefore, only signals belonging to  
346 HPMC block are detected. Signals corresponding to PLLA block are not detected because of  
347 the limited molecular motion in aqueous medium, which is consistent with the formation of  
348 micelles with a hydrophilic HPMC shell and a hydrophobic PLLA core.

349         Similar to low molar mass surfactants, the self-assembly of the amphiphilic copolymers  
350 occurs when the concentration reaches the CMC. The latter is an important parameter of  
351 amphiphilic copolymers as it determines the stability of micelles. In the case of drug delivery  
352 systems, drug loaded micelles should remain stable with dilution after intravenous injection.  
353 In this work, the CMC was determined from scattering intensity changes of copolymer  
354 solutions as a function of concentration. At low concentrations, the scattered intensity is very  
355 low because of the absence of nano-objects. With increasing concentration, the intensity  
356 strongly increases due to the formation of nano-micelles. The CMC value is obtained from the  
357 crossover point of the two regression lines. As shown in Table 1, the CMC of (HPMC10K)<sub>2</sub>-  
358 PLA2K, (HPMC7K)<sub>2</sub>-PLA2K, and (HPMC5K)<sub>2</sub>-PLA2K copolymers is 0.16, 0.15, and 0.14 g  
359 L<sup>-1</sup>, respectively. These values well agree with the reported CMC value 0.13 mg/mL for  
360 cellulose-*g*-polylactide (Guo et al., 2012). Obviously the CMC increases with the hydrophilic  
361 ratio or the HPMC block length as the self-assembly of neutral block copolymers is mainly  
362 determined by the hydrophilic/hydrophobic balance (Larue et al., 2008).

363 The self-assembled (HPMC)<sub>2</sub>-PLA micelles are composed of a PLA core surrounded by  
364 a HPMC corona. The average diameter of (HPMC5K)<sub>2</sub>-PLA2K, (HPMC7K)<sub>2</sub>-PLA2K,  
365 (HPMC10K)<sub>2</sub>-PLA2K micelles was 66, 90 and 120 as determined by DLS, as shown in Table  
366 1. All the micelles exhibited a unimodal size distribution, and the PDI was in the range of 0.12  
367 to 0.21. Thus, the micelle size of copolymers increases with the increase of hydrophilic  
368 HPMC chain length, in agreement with literature. In our previous work, the average micelle  
369 size of HPMC5K-PLA2K, HPMC8K-PLA2K, HPMC10K-PLA2K diblock copolymers was  
370 62, 96, 120 nm, respectively (Wang et al., 2017). Thus, micelles of (HPMC5K)<sub>2</sub>-PLA2K had  
371 a smaller size compared to HPMC10K-PLA2K with the same hydrophilic/hydrophobic  
372 balance but a Y-type topology. It has been reported that the chain architecture affects the  
373 micellization properties, including the aggregation number, size, polydispersity, and micelle  
374 density (Liu et al., 2007). Generally, the micelle size of multiple-arm copolymers is smaller  
375 than that of linear ones. Meanwhile, micelles with the same HPMC block length but different  
376 topologies had almost the same size. This finding could be attributed to the fact that the core  
377 is composed of the same PLA blocks, and the corona of similar HPMC chains although the  
378 chain density should be higher for Y-type copolymers.

379



380

381 Figure 7. TEM images of (HPMC)<sub>2</sub>-PLA micelles in water: (A) (HPMC5K)<sub>2</sub>-PLA2K; (B)

382

(HPMC7K)<sub>2</sub>-PLA2K; (C) (HPMC10K)<sub>2</sub>-PLA2K.

383

384 The morphology of (HPMC)<sub>2</sub>-PLA micelles was characterized by using TEM. Figure 7  
385 shows that the micelles were spherical in shape and uniformly distributed. The observed  
386 micelle size increased with the increasing of the HPMC chain length, which well agreed with  
387 the results obtained by DLS.

388

#### 389 4. Conclusion

390 AB<sub>2</sub>-type amphiphilic block copolymers (HPMC)<sub>2</sub>-PLA with three different HPMC  
391 block lengths were synthesized by ring opening polymerization, reductive amination and click  
392 reaction. The copolymers were characterized by using various methods, including NMR,  
393 DOSY-NMR, SEC and FT-IR. The cloud point of AB<sub>2</sub>-type (HPMC)<sub>2</sub>-PLA are nearly 64 °C,  
394 which is obviously lower than HPMC oligomers and linear HPMC-b-PLA diblock  
395 copolymers. The HPMC block length has little effect the Cp value. (HPMC)<sub>2</sub>-PLA  
396 copolymers can self-assemble to form spherical micelles with narrow distribution. The size of  
397 copolymer micelles increases with the increase of HPMC fraction. So does the CMC of  
398 (HPMC)<sub>2</sub>-PLA. It is thus concluded that biobased and biodegradable HPMC-PLA copolymers  
399 could be promising as nano-carrier of hydrophobic drugs.

400

401 **Keywords:** Hydroxypropyl methyl cellulose; Poly(L-lactide); Topology; Self-assembly;

402 Micelle

403

#### 404 **Acknowledgements**

405 This work is supported in part by the scholarship from China Scholarship Council (CSC)  
406 under the Grant CSC N°201606240124.

407

## 408 **References**

- 409 Aminabhavi, T. M., Nadagouda, M. N., Joshi, S. D., & More, U. A. (2014). Guar gum as platform for the oral  
410 controlled release of therapeutics. *Expert Opin Drug Deliv*, 11(5), 753-766.
- 411 Barz, M., Luxenhofer, R., Zentel, R., & Vicent, M. J. (2011). Overcoming the PEG-addiction: well-defined  
412 alternatives to PEG, from structure–property relationships to better defined therapeutics.  
413 *Polymer Chemistry*, 2(9), 1900.
- 414 Cao, J., Lu, A., Li, C., Cai, M., Chen, Y., Li, S., & Luo, X. (2013). Effect of architecture on the micellar  
415 properties of poly (varepsilon-caprolactone) containing sulfobetaines. *Colloids Surf B*  
416 *Biointerfaces*, 112, 35-41.
- 417 Chen, D., & Sun, B. (2000). New tissue engineering material copolymers of derivatives of cellulose and  
418 lactide: their synthesis and characterization. *Materials Science and Engineering: C*, 11(1), 57-60.
- 419 Claes, M. (2006). New Methods for Enzyme Hydrolysis, Analysis, and Characterization of Modified  
420 Cellulose. *Analytical Chemistry* (Vol. Ph.D, p. 180). Lund: Lund University.
- 421 Elsbahy, M., & Wooley, K. L. (2012). Design of polymeric nanoparticles for biomedical delivery  
422 applications. *Chem Soc Rev*, 41(7), 2545-2561.
- 423 Fitzpatrick, F., Schagerlöf, H., Andersson, T., Richardson, S., Tjerneld, F., Wahlund, K.-G., & Wittgren, B.  
424 (2006). NMR, Cloud-Point Measurements and Enzymatic Depolymerization: Complementary Tools  
425 to Investigate Substituent Patterns in Modified Celluloses. *Biomacromolecules*, 7(10), 2909-2917.
- 426 Ganguly, K., Chaturvedi, K., More, U. A., Nadagouda, M. N., & Aminabhavi, T. M. (2014). Polysaccharide-  
427 based micro/nanohydrogels for delivering macromolecular therapeutics. *J Control Release*, 193,  
428 162-173.
- 429 Guo, Y., Wang, X., Shen, Z., Shu, X., & Sun, R. (2013). Preparation of cellulose-graft-poly(varepsilon-  
430 caprolactone) nanomicelles by homogeneous ROP in ionic liquid. *Carbohydr Polym*, 92(1), 77-83.
- 431 Guo, Y., Wang, X., Shu, X., Shen, Z., & Sun, R. C. (2012). Self-assembly and paclitaxel loading capacity of  
432 cellulose-graft-poly(lactide) nanomicelles. *J Agric Food Chem*, 60(15), 3900-3908.
- 433 Honda, S., Yamamoto, T., & Tezuka, Y. (2010). Topology-directed control on thermal stability: micelles  
434 formed from linear and cyclized amphiphilic block copolymers. *J Am Chem Soc*, 132(30), 10251-  
435 10253.
- 436 Hsieh, M.-F., Van Cuong, N., Chen, C.-H., Chen, Y. T., & Yeh, J.-M. (2008). Nano-Sized Micelles of Block  
437 Copolymers of Methoxy Poly(ethylene glycol)-Poly(ε-caprolactone)-Graft-2-  
438 Hydroxyethyl Cellulose for Doxorubicin Delivery. *Journal of Nanoscience and Nanotechnology*,  
439 8(5), 2362-2368.
- 440 Huo, M., Zou, A., Yao, C., Zhang, Y., Zhou, J., Wang, J., . . . Zhang, Q. (2012). Somatostatin receptor-  
441 mediated tumor-targeting drug delivery using octreotide-PEG-deoxycholic acid conjugate-  
442 modified N-deoxycholic acid-O, N-hydroxyethylation chitosan micelles. *Biomaterials*, 33(27),  
443 6393-6407.
- 444 Ishida, T., & Kiwada, H. (2008). Accelerated blood clearance (ABC) phenomenon upon repeated injection

445 of PEGylated liposomes. *Int J Pharm*, 354(1-2), 56-62.

446 Jeong, Y. I., Kim, D. H., Chung, C. W., Yoo, J. J., Choi, K. H., Kim, C. H., . . . Kang, D. H. (2011). Doxorubicin-  
447 incorporated polymeric micelles composed of dextran-b-poly(DL-lactide-co-glycolide) copolymer.  
448 *Int J Nanomedicine*, 6, 1415-1427.

449 Jeong, Y. I., Na, H. S., Oh, J. S., Choi, K. C., Song, C. E., & Lee, H. C. (2006). Adriamycin release from self-  
450 assembling nanospheres of poly(DL-lactide-co-glycolide)-grafted pullulan. *Int J Pharm*, 322(1-2),  
451 154-160.

452 Kataoka, K., Harada, A., & Nagasaki, Y. (2001). Block copolymer micelles for drug delivery: design,  
453 characterization and biological significance. *Adv Drug Deliv Rev*, 47(1), 113-131.

454 Khan, I. A., Anjum, K., Koya, P. A., Qadeer, A., & Kabir ud, D. (2014). Cloud point, fluorimetric and <sup>1</sup>H NMR  
455 studies of ibuprofen-polymer systems. *Journal of Molecular Structure*, 1056-1057, 254-261.

456 Kostanski, L. K., Keller, D. M., & Hamielec, A. E. (2004). Size-exclusion chromatography-a review of  
457 calibration methodologies. *J Biochem Biophys Methods*, 58(2), 159-186.

458 Larue, I., Adam, M., Zhulina, E. B., Rubinstein, M., Pitsikalis, M., Hadjichristidis, N., . . . Sheiko, S. S. (2008).  
459 Effect of the soluble block size on spherical diblock copolymer micelles. *Macromolecules*, 41(17),  
460 6555-6563.

461 Lassalle, V., & Ferreira, M. L. (2007). PLA nano- and microparticles for drug delivery: an overview of the  
462 methods of preparation. *Macromol Biosci*, 7(6), 767-783.

463 Li, Z., Kesselman, E., Talmon, Y., Hillmyer, M. A., & Lodge, T. P. (2004). Multicompartment micelles from  
464 ABC miktoarm stars in water. *Science*, 306(5693), 98-101.

465 Liu, H., Xu, J., Jiang, J., Yin, J., Narain, R., Cai, Y., & Liu, S. (2007). Syntheses and micellar properties of well-  
466 defined amphiphilic AB<sub>2</sub> and A<sub>2</sub>B Y-shaped miktoarm star copolymers of ε-caprolactone and 2-  
467 (dimethylamino)ethyl methacrylate. *Journal of Polymer Science Part A: Polymer Chemistry*, 45(8),  
468 1446-1462.

469 Mi, P., Wang, F., Nishiyama, N., & Cabral, H. (2017). Molecular Cancer Imaging with Polymeric  
470 Nanoassemblies: From Tumor Detection to Theranostics. *Macromol Biosci*, 17(1).

471 Muller, J., Marchandea, F., PreLOT, B., Zajac, J., Robin, J.-J., & Monge, S. (2015). Self-organization in water  
472 of well-defined amphiphilic poly(vinyl acetate)-b-poly(vinyl alcohol) diblock copolymers. *Polymer*  
473 *Chemistry*, 6(16), 3063-3073.

474 Ostmark, E., Nystrom, D., & Malmstrom, E. (2008). Unimolecular nanocontainers prepared by ROP and  
475 subsequent ATRP from hydroxypropylcellulose. *Macromolecules*, 41(12), 4405-4415.

476 Pages, G., Gilard, V., Martino, R., & Malet-Martino, M. (2017). Pulsed-field gradient nuclear magnetic  
477 resonance measurements (PFG NMR) for diffusion ordered spectroscopy (DOSY) mapping.  
478 *Analyst*, 142(20), 3771-3796.

479 Rajendra P. Pawara, S. U. T., Suresh U. Shisodiaa, Jalinder T. Totrea and, & Abraham J. Dombb. (2014).  
480 Biomedical Applications of Poly(Lactic Acid). *Recent Patents on Regenerative Medicine*, 4, 40-51.

481 Ramzi A. Abd Alsaheb, A. A., Nor Zalina Othman, Roslinda Abd Malek, Ong Mei Leng, Ramlan Aziz<sup>1</sup> and  
482 Hesham A. El Enshasy. (2015). Recent applications of polylactic acid in pharmaceutical and  
483 medical industries. *Journal of Chemical and Pharmaceutical Research*, 7(12), 51-63.

484 Rancan, F., Papakostas, D., Hadam, S., Hackbarth, S., Delair, T., Primard, C., . . . Vogt, A. (2009).  
485 Investigation of Polylactic Acid (PLA) Nanoparticles as Drug Delivery Systems for Local  
486 Dermatotherapy. *Pharmaceutical Research*, 26(8), 2027-2036.

487 Rudzinski, W. E., & Aminabhavi, T. M. (2010). Chitosan as a carrier for targeted delivery of small interfering  
488 RNA. *Int J Pharm*, 399(1-2), 1-11.



489 Saini, P., Arora, M., & Kumar, M. (2016). Poly(lactic acid) blends in biomedical applications. *Adv Drug Deliv*  
490 *Rev*, 107, 47-59.

491 Sardar, N., Kamil, M., Kabir ud, D., & Sajid Ali, M. (2011). Solution Behavior of Nonionic Polymer  
492 Hydroxypropylmethyl Cellulose: Effect of Salts on the Energetics at the Cloud Point. *Journal of*  
493 *Chemical & Engineering Data*, 56(4), 984-987.

494 Schatz, C., & Lecommandoux, S. (2010). Polysaccharide-Containing Block Copolymers: Synthesis,  
495 Properties and Applications of an Emerging Family of Glycoconjugates. *Macromolecular Rapid*  
496 *Communications*, 31(19), 1664-1684.

497 Sun, H., Guo, B., Cheng, R., Meng, F., Liu, H., & Zhong, Z. (2009). Biodegradable micelles with sheddable  
498 poly(ethylene glycol) shells for triggered intracellular release of doxorubicin. *Biomaterials*, 30(31),  
499 6358-6366.

500 Teramoto, Y., & Nishio, Y. (2003). Cellulose diacetate-graft-poly(lactic acid)s: synthesis of wide-ranging  
501 compositions and their thermal and mechanical properties. *Polymer*, 44(9), 2701-2709.

502 Tian, J. L., Zhao, Y. Z., Jin, Z., Lu, C. T., Tang, Q. Q., Xiang, Q., . . . Zhang, Y. (2010). Synthesis and  
503 characterization of Poloxamer 188-grafted heparin copolymer. *Drug Dev Ind Pharm*, 36(7), 832-  
504 838.

505 Tsuji, H. (2005). Poly(lactide) stereocomplexes: formation, structure, properties, degradation, and  
506 applications. *Macromol Biosci*, 5(7), 569-597.

507 Wang, J., Caceres, M., Li, S., & Deratani, A. (2017). Synthesis and Self-Assembly of Amphiphilic Block  
508 Copolymers from Biobased Hydroxypropyl Methyl Cellulose and Poly(l  
509 -lactide). *Macromolecular Chemistry and Physics*, 218(10), 1600558.

510 Yang, L., Wu, X., Liu, F., Duan, Y., & Li, S. (2009). Novel biodegradable polylactide/poly(ethylene glycol)  
511 micelles prepared by direct dissolution method for controlled delivery of anticancer drugs. *Pharm*  
512 *Res*, 26(10), 2332-2342.

513 Yang, Y. L., Kataoka, K., & Winnik, F. M. (2005). Synthesis of diblock copolymers consisting of hyaluronan  
514 and poly(2-ethyl-2-oxazoline). *Macromolecules*, 38(6), 2043-2046.

515 Yi, Y., Lin, G., Chen, S., Liu, J., Zhang, H., & Mi, P. (2018). Polyester micelles for drug delivery and cancer  
516 theranostics: Current achievements, progresses and future perspectives. *Mater Sci Eng C Mater*  
517 *Biol Appl*, 83, 218-232.

518 You, Y. Z., Hong, C. Y., Wang, W. P., Lu, W. Q., & Pan, C. Y. (2004). Preparation and characterization of  
519 thermally responsive and biodegradable block copolymer comprised of PNIPAAm and PLA by  
520 combination of ROP and RAFT methods. *Macromolecules*, 37(26), 9761-9767.

521 Yuan, W., Yuan, J., Zhang, F., & Xie, X. (2007). Syntheses, characterization, and in vitro degradation of ethyl  
522 cellulose-graft-poly(epsilon-caprolactone)-block-poly(L-lactide) copolymers by sequential ring-  
523 opening polymerization. *Biomacromolecules*, 8(4), 1101-1108.

524